

Relationship between the dielectric properties and the conductivity of $\text{Ba}_2\text{FeNbO}_6$

X. H. Sun · C. C. Wang · G. J. Wang · C. M. Lei · T. Li ·
J. Y. Mei · Y. M. Cui

Received: 28 November 2011 / Accepted: 24 August 2012 / Published online: 5 September 2012
© Springer Science+Business Media, LLC 2012

Abstract In the present work, we performed detailed investigation on the relationship between the dielectric properties and the conductivity of $\text{Ba}_2\text{FeNbO}_6$. Our results revealed that (1) the colossal dielectric behavior of the sample can be well understood based on the framework of universal dielectric response, (2) the observed relaxation shows a distinct deviation from the Arrhenius behavior, and (3) the peak intensity of dielectric loss can be well expressed by a relation similar to the Fermi–Dirac distribution function rather than a thermally activation relation. These are the typical features for the hopping motions of polaronic carriers demonstrating that the dielectric properties and the conductivity of $\text{Ba}_2\text{FeNbO}_6$ are closely linked.

Keywords Ceramics · Dielectric properties · Polaron relaxation

1 Introduction

$\text{Ba}_2\text{FeNbO}_6$ (BFN) was first synthesized via solid state reaction technique by Saha and Sinha in 2002 [1]. This material has soon attracted considerable interest because several groups assumed that BFN is a lead-free ferroelectric-relaxor as the material exhibits diffuse phase transition dielectric behavior in the temperature range around 200 °C [1–6]. While

other group attributed the high-temperature relaxer-like dielectric to oxygen defect induced dielectric abnormality [7]. In spite of this dispute, the most interesting property is that BFN shows similar colossal dielectric behavior to that observed in $\text{CaCu}_3\text{Ti}_4\text{O}_{12}$ (CCTO) in the temperature range below room temperature [4]. Raevski et al. [4] attributed the low temperature (LT) dielectric relaxation in BFN to a Maxwell–Wagner (M–W) relaxation. Ramirez et al. [8] argued that the M–W mechanism cannot solely responsible for such LT relaxation in CCTO and the analog materials exhibiting colossal dielectric constants. Recently Ke et al. [9] investigated both low and high temperature dielectric relaxations in BFN. The high temperature dielectric relaxation was considered as a competitive phenomenon between the dielectric relaxation and electrical conduction of the relaxing species, whereas the LT relaxation was ascribed to be a polaronic relaxation. The existing results show that the physical mechanisms of both the low- and high-temperature dielectric responses in BFN are far from well understood. In the present work, we have performed detailed investigation on the LT dielectric behavior of BFN. Our results demonstrate a clear relationship between the observed dielectric properties and the conductivity. This implies that the relaxation in BFN might be a dipolar-type relaxation associated with the hopping localized carriers.

2 Experimental

The samples were prepared by the standard solid-state reaction technique. Stoichiometric amount of BaCO_3 , Fe_2O_3 and Nb_2O_5 (all of 4N grade) powders were thoroughly mixed using a mortar and calcined at 1200 °C for 24 h. This procedure was repeated three times with intermediate grindings. The resultant powder was reground and pressed into pellets and finally sintered at 1350 °C for 10 h followed by furnace cooling to room temperature. Phase purity of sintered pellets was characterized by X-ray powder diffraction

X. H. Sun · C. C. Wang (✉) · G. J. Wang · C. M. Lei · T. Li ·
J. Y. Mei
Laboratory of Dielectric Functional Materials,
School of Physics and Material Science, Anhui University,
Hefei 230039, People's Republic of China
e-mail: ccwang@ahu.edu.cn

Y. M. Cui
Key Laboratory of Micro-nano Measurement-Manipulation and
Physics (Ministry of Education), Department of Physics,
Beihang University,
Beijing 100191, People's Republic of China

performed on a MXP18AHF diffractometer (MARK, Japan) with Cu K α radiation. Microstructure and grain size of the sintered pellets were studied by a field emission scanning electron microscope (SEM) (Model S-4800, Hitachi Co., Tokyo, Japan). Electrodes were made by printing silver paste on both sides of the disk-type samples and then two fine copper wires used as down-lead were connected to the printed sides. The temperature dependent dielectric properties were obtained using a HIOKI 3532-50 LCR precise impedance analyzer with the sample connected to a measuring rod and inserted into a container with liquid nitrogen. The dielectric measurements were carried out in the frequency range from 100 Hz to 1 MHz. The system can provide a temperature range from 76 to 335 K controlled by a Lakeshore 331 temperature controller. The amplitude of ac measuring signal was 100 mV rms. Annealing treatments were performed in flowing (200 ml/min) N₂ and O₂ (both with purity >99.999 %).

3 Results and discussion

The X-ray diffraction pattern of the as-prepared BFN ceramic sample is shown in Fig. 1. The pattern was analyzed using Jade 5 power diffraction data analysis software. It was found that the pattern can be indexed to a cubic structure. The calculated lattice constant $a=8.11968$ Å is fairly consistent with that reported by Ke et al. (8.11 Å) [9]. The typical SEM micrograph of BFN is shown in the inset of Fig. 1. The micrograph indicates that the pellet was dense and compact with an average grain size about 20 μm . The as-prepared sample achieves density of 6.18 g/cm³, which is about 94.88 % of the theoretical value (6.51 g/cm³).

Figure 2 compares the temperature (T) dependence of the real (ϵ' , left panels) and imaginary (ϵ'' , right panels) parts of

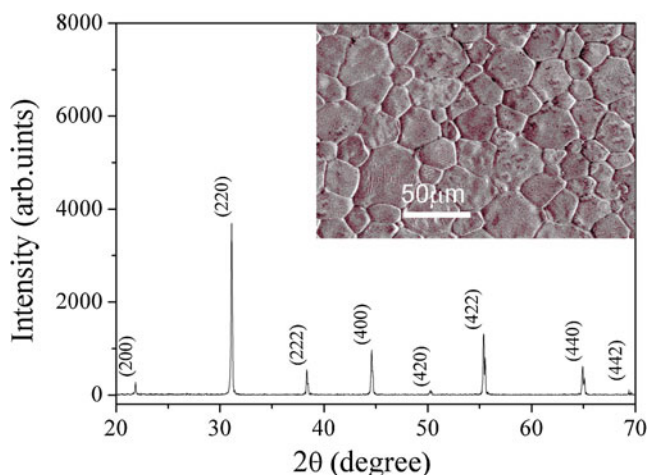


Fig. 1 The XRD pattern and SEM image obtained at room temperature of the BFN ceramics

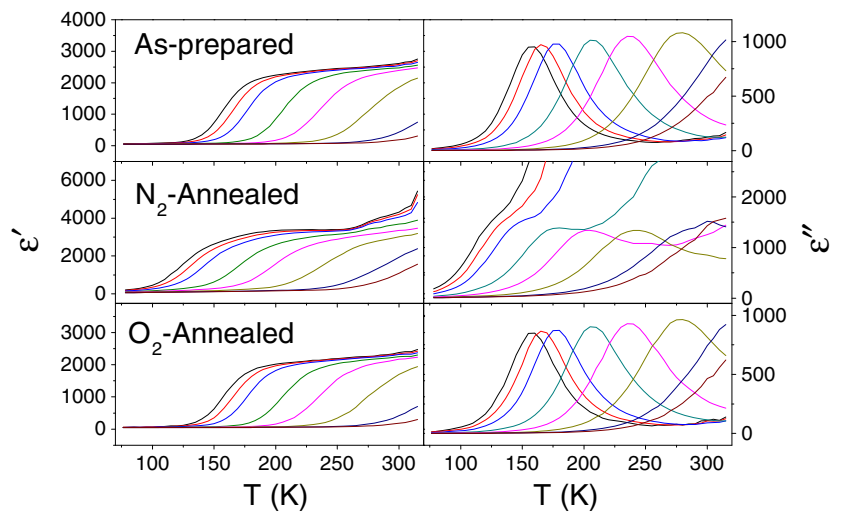
the complex permittivity at a number of representative frequencies for BFN before (as-prepared) and after post-annealing processes at N₂ and O₂ atmospheres. It can be seen that the low-temperature dielectric behavior of BFN exhibits similar features to those found in CCTO [10]. That is, $\epsilon'(T)$ shows high values with weak temperature-dependent at high temperatures. As the temperature decreases to a critical temperature depending on the measuring frequency, $\epsilon'(T)$ step-like decreases to a flat range which almost independent of frequency. The step-like decrease in $\epsilon'(T)$ is accompanied by a peak in the corresponding curve of $\epsilon''(T)$. Although the mechanism of these features in CCTO is still an open question, it was reported that they are closely related to oxygen vacancy [11, 12]. To check out whether or not the dielectric properties in BFN is related to oxygen vacancy, we performed annealing treatments firstly in nitrogen and then in oxygen atmospheres at 800 °C for 2 h. After each treatment, dielectric properties were measured as a function of temperature. We note that annealing in N₂ atmosphere leads to a significant enhancement of dielectric constant; and the relaxation moves to lower temperature by ~18 K. Additionally, the relaxation peak in $\epsilon''(T)$ measured with low frequencies was found to superimpose upon a nearly exponential increasing background. Whereas after the consecutive annealing in O₂, both $\epsilon'(T)$ and $\epsilon''(T)$ return back to almost the same levels as those of the as-prepared case. These results exclusively demonstrate that the low-temperature dielectric properties of BFN are truly related to oxygen vacancy. The oxygen vacancies actually act as donors that can yield conductive electrons. Because the dielectric loss ($\epsilon''(T)$) related to conductivity (σ) can be written as $\epsilon'' \propto \sigma/\omega \propto \exp(-E_{\text{cond}}/k_B T)/\omega$ [13] with k_B the Boltzmann constant, E_{cond} the activation energy of the conductivity and ω the angular frequency. This is the reason why a nearly exponential increasing background was observed. The above results imply an intimate relationship between the observed dielectric properties and the conductivity produced by oxygen vacancies.

Now we focus our attention on the relationship between the two aspects. Firstly, it is well known that in semiconducting materials, localized charge carriers hopping between spatially fluctuating lattice potentials not only produce conductivity but also give rise to dipolar effects. The frequency dependent dielectric response caused by the localized carriers can be described by Jonscher's power law [14], i.e., the universal dielectric response (UDR). This model predicts a frequency-dependent ac conductivity of ω^s , which yields a ω^{s-1} behavior for the dielectric constant by the Kramers-Kronig transformation. Then, one has

$$f\epsilon' = A(T)f^s \quad (1)$$

where $A(T)$ and s (with values between 0 and 1) are the temperature-dependent constants, $f=\omega/2\pi$ is the testing

Fig. 2 Temperature dependence of ϵ' (left panels) and ϵ'' (right panels) at a number of representative frequencies for BFN before (as-prepared) and after N₂ and O₂ annealing treatments. The measuring frequencies are 300, 500, 1000, 5000, 20 000, 100 000, 500 000, 1000 000 Hz (from left to right)



frequency. Therefore, at a given temperature, a straight line with the slope of s should be obtained in the plot of $\log_{10} f \epsilon'$ versus $\log_{10} f$. Figure 3 presents such a plot for the as-prepared BFN sample, from which perfect straight lines with almost common slope of $s=0.979$ in the high-temperature and low-frequency ranges were observed. The experimental data in the high-frequency range deviate from the straight line, because of the occurrence of the relaxation that causes a steplike decrease in ϵ' (see Fig. 2). The deviation gradually shifts to lower frequencies as the relaxation moves to lower frequencies with decreasing temperature. As the relaxation moves to low frequencies, straight line appears again in the high-frequency range at low temperatures with nearly same slope of $s=0.997$. The value of $s=0.997 \approx 1$ at low temperatures indicates that the related carriers are strictly localized [15]. This means the carriers are frozen ones that they cannot hop and no longer have contribution to neither conductivity nor dielectric response. Therefore, the observed

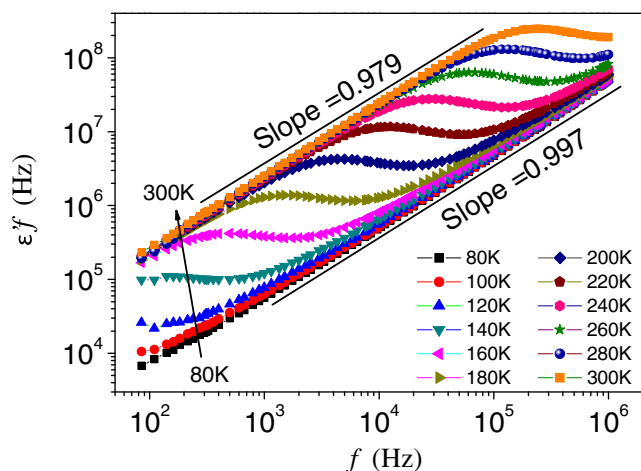


Fig. 3 Plots of $\log_{10} (f \epsilon')$ vs $\log_{10} (f)$ for BFN at a number of fixed temperatures. The solid linear lines are guides for the eyes

dielectric constant and dielectric loss become flat values. This is virtually a nearly constant loss behavior [16]. From $s=0.979$ at 300 K to $s \approx 1$ at 80 K, the involved charge carriers are more and more localized. This means that their inertial mass (or eigenfrequency) becomes sufficiently large (low). Then, they cannot follow the field variations and the resulting effect is a dielectric relaxation with the relaxation peak appearing at the temperature where the eigenfrequency of the carriers equals the frequency of the applied field. Therefore, the observed relaxation can be ascribed to the hopping localized carriers.

Secondly, let's check out the Arrhenius relation, i.e., the testing frequency as a function of the inverse peak temperature (T_p) in dielectric loss $\epsilon''(T)$. Figure 4 displays the Arrhenius plots for BFN sample measured in difference

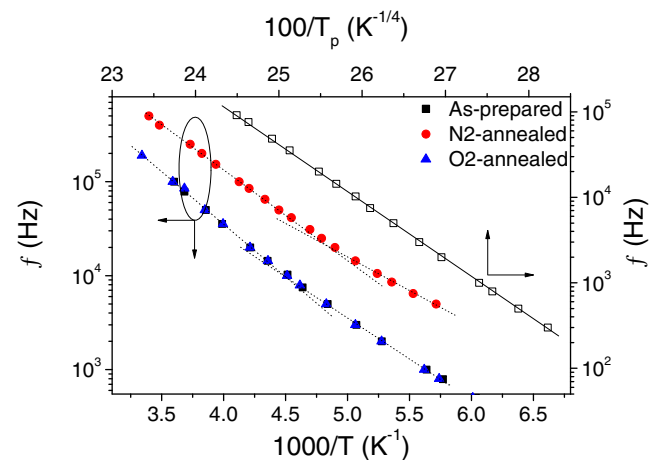


Fig. 4 The panel with bottom and left axes shows the Arrhenius plots of $\log_{10} f$ vs $1/T_p$ for BFN before (as-prepared) and after O₂ and N₂ annealing treatments. Dotted lines illustrate two Arrhenius segments. The panel with top and right axes replots the same data for the as-prepared sample in terms of the VRH-like relation. The solid line is the results of liner fit based on Eq. (2)

cases. We note that (i) The data obtained in the cases of the as-prepared and after O₂-annealing treatment are almost overlap, convincing that both cases have almost the same dielectric behavior. (ii) A distinct deviation from the Arrhenius behavior is observed for BFN in both the as-prepared and the annealed cases. A tentative explanation to this deviation as suggested by Grubbs et al. is that the investigated sample might contain two relaxations with different activation energies leading to two Arrhenius segments as illustrated by the dotted lines in the figure [17]. But this inference can be easily ruled out; since if it was true, both relaxations rather than only one relaxation should appear in the high (low)-frequency (temperature) range. Zhang and Tang [18] that suggested that the Mott’s variable range hopping (VRH) relation fit the data better for relaxation in CCTO:

$$f = f_0 \exp\left[(T_0/T_P)^{1/4}\right] \tag{2}$$

where f_0 is the eigenfrequency and T_0 is a constant related to the activation energy. Although the VRH relation truly gives a very good straight line as shown in the same panel of the figure, which yields unrealistic parameter $f_0 = 6.02 \times 10^{22}$ Hz [19].

The polaronic model does provide a heuristic hint to understand the deviation. In the polaronic scenario [20], thermally activated hopping conductivity obeys the following equation

$$\sigma = T^{-1} \exp(-W/k_B T) \tag{3}$$

The activation energy W for the small-polaron is given by [21] $W = W_H + 1/2W_D$ in the high-temperature range (where W_H and W_D are the hopping and disorder energy, respectively); while in the low-temperature range $W \approx W_D$. For polarons, the relaxation behavior is dominated by the

conductivity behavior [19]. The change of activation energy for conductivity will lead to the change of activation energy for dielectric relaxation, thereby, giving rise to the deviation of the Arrhenius plot. This further demonstrates that the conductivity and the relaxation are closely related.

Finally, for the polaron relaxation, the peak intensity of dielectric loss is proportional to the concentration of relaxation units [22]

$$\varepsilon''_{\max} = N\mu^2/3\varepsilon_0k_B T \tag{4}$$

where μ is the dipole moment, N is the concentration of the hopping polarons, and ε_0 is the dielectric permittivity of free space. N was usually reported to vary with the temperature following a thermally activated relation [23]

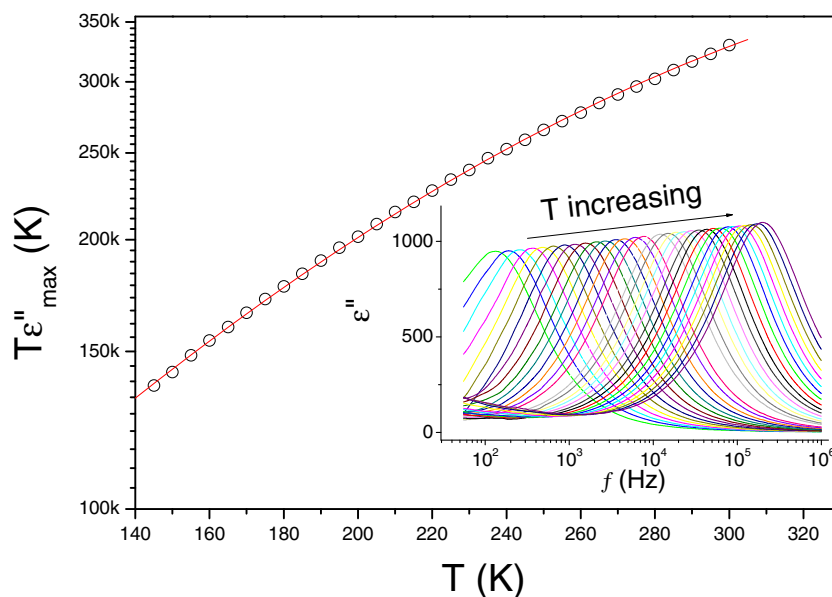
$$N = N_0 \exp(-E/k_B T) \tag{5}$$

where N_0 is the pre-exponential factor representing the concentration of polaron at $T \rightarrow \infty$ and E is the activation energy. One thus has:

$$T\varepsilon''_{\max} = N_0 \exp(-E/k_B T)\mu^2/3k_B \tag{6}$$

In order to verify the validity of Eq. 6, $\varepsilon''(f)$ for the as-prepared sample was measured at series of temperatures from 145 K to 300 K varying with 5 K increment (inset of Fig. 5). The peak intensity was found to gradually increase as the peak shifts to high frequencies. But it cannot be fitted by the thermally activated behavior as expressed by Eq. 6. This might because that the observed dielectric relaxation is associated with a frozen-in process of hopping polarons. Like that in canonical glasses, this process should exist a finite temperature, T_f to manifest the freezing temperature. In our previous paper, a relation similar to the Fermi–Dirac distribution function was suggested to describe the concentration of the frozen carriers

Fig. 5 Temperature dependence of $T\varepsilon''_{\max}$ for the as-prepared BFN sample. *Solid line* is the fitting result base on Eqs. (4) and (7). Inset shows the frequency dependence of ε'' at temperatures varying from 145 to 300 K with 5 K increment



[24]. Hence, the concentration of the hopping polarons can be written as [25]

$$N = N_0(1 - 1/(\exp((T - T_f)/\Delta) + 1)) \quad (7)$$

where T_f is the most probable freezing temperature, and Δ is the parameter describing the width of freezing temperatures. Taking Eqs. (4) and (7), the experimental data can be perfectly fitted. The result of the fit is given as a solid line in the main panel of Fig. 5. The fit yields $T_f=243$ K, $\Delta=98$ K, and $N_0\mu^2/3\varepsilon_0k_B=512,847$ K. The last parameter is related to the number of polarons per unit volume, which is of vital importance in semiconductor science. The attempt to deduce this number needs microscopic information about the dipole. If we assume the dipole is composed of opposite carriers carrying a charge of 1.6×10^{-19} C and separating by the distance of one lattice parameter, the polaron concentration at high temperature limit is found to be $10^{22}/\text{cm}^3$. This value is reasonable considering the typical concentration for most semiconductors is in the range of 10^{16} – $10^{21}/\text{cm}^3$ at room temperature. This fact evidences that the dielectric properties of BFN and the conductivity are closely linked.

4 Conclusions

In summary, the dielectric properties of BFN ceramics were investigated as functions of temperature ($80 \text{ K} \leq T \leq 320 \text{ K}$) and frequency ($100 \text{ Hz} \leq f \leq 1 \text{ MHz}$). Our results indicate that the dielectric properties and the conductivity of BFN are closely linked. The observed dielectric properties can be well understood based on the polaron model suggesting that the relaxation in BFN can be ascribed to a dipolar relaxation associated with the hopping motions of the polaronic carriers.

Acknowledgments The authors gratefully thank S.Y. Lu and Z. Q. Lin at the Modern Experiment Technology Center of Anhui University for their help in XRD and SEM experiments. We acknowledge financial support from National Natural Science Foundation of China under Grant No 11074001.

References

1. S. Saha, T.P. Sinha, J. Phys. Condens. Matter **14**, 249 (2002)
2. I.P. Raevski, S.A. Kuropatkina, S.P. Kubrin, S.I. Raevskaya, V.V. Titov, D.A. Sarychev, M.A. Malitskaya, A.S. Bogayin, I.N. Zakharchenko, Ferroelectrics **379**, 48 (2009)
3. C.Y. Chung, Y.H. Chang, G.J. Chen, Y.L. Chai, J. Cryst. Growth **284**, 100 (2005)
4. I.P. Raevski, S.A. Prosandeev, A.S. Bogatin, M.A. Malitskaya, L. Jastrabik, J. Appl. Phys. **93**, 4130 (2003)
5. D. Bochenek, Z. Surowiak, J. Poltirova-Vejpravova, J. Alloys Compd. **487**, 572 (2009)
6. U. Intatha, S. Eitssayeam, K. Pengpat, K.J.D. MacKenzie, T. Tunkasiri, Mater. Lett. **61**, 196 (2007)
7. Z. Wang, X.M. Chen, L. Ni, X.Q. Liu, Appl. Phys. Letts. **90**, 022904 (2007)
8. A.P. Ramirez, M.A. Subramanian, M. Gardel, G. Blumberg, D. Li, T. Vogt, S.M. Shapiro, Solid State Commun. **115**, 217 (2000)
9. S. Ke, H.Q. Fan, H.T. Huang, J. Electroceram. **22**, 252 (2009)
10. M.A. Subramanian, D. Li, N. Duan, B.A. Reisner, A.W. Sleight, J. Solid State Chem. **151**, 323 (2000)
11. C.C. Wang, L.W. Zhang, Appl. Phys. Letts. **88**, 042906 (2006)
12. M.A. Pires, C. Israel, W. Iwamoto, R.R. Urbano, O. Agüero, I. Torriani, C. Rettori, P.G. Pagliuso, L. Walmsley, Z. Le, J.L. Cohn, S.B. Oseroff, Phys. Rev. B **73**, 224404 (2006)
13. C.C. Wang, Y.M. Cui, L.W. Zhang, Appl. Phys. Letts. **90**, 012904 (2007)
14. A.K. Jonscher, *Dielectric Relaxation in Solids* (Chelsea, London, 1983)
15. A.S. Nowick, B.S. Lim, Phys. Rev. B **63**, 184115 (2001)
16. A.S. Nowick, A.V. Vaysleyb, I. Kuskovsky, Phys. Rev. B **58**, 8398 (1998)
17. R.K. Grubbs, E.L. Venturini, P.G. Clem, J.J. Richardson, B.A. Tuttle, G.A. Samara, Phys. Rev. B **72**, 104111 (2005)
18. L. Zhang, Z.J. Tang, Phys. Rev. B **70**, 174306 (2004)
19. C.C. Wang, L.W. Zhang, Appl. Phys. Letts. **90**, 142905 (2007)
20. N.F. Mott, E.A. Davis, *Electric Process in Non-Crystalline Materials* (Clarendon, Oxford, 1979)
21. W.H. Jung, H. Nakatsugawa, E. Iguchi, J. Solid State Chem. **133**, 466 (1997)
22. L.L. Hench, J.K. West, *Principles of Electronic Ceramics* (Wiley, New York, 1990)
23. S. Komine, E. Iguchi, J. Phys. Condens. Matter **16**, 1061 (2004)
24. C.C. Wang, L.W. Zhang, Appl. Phys. Letts. **92**, 132903 (2008)
25. C.C. Wang, X. Zheng, J. Zhu, Mater. Letts. **58**, 1237 (2004)